Interference Driven Antenna Selection for Massive Multi-User MIMO

Pierluigi V. Amadori, *Student Member, IEEE*, and Christos Masouros, *Senior Member, IEEE*

***Abstract*—Low-complexity linear precoders are known to be close-to-optimal for massive multi-input multi-output (M-MIMO) systems. However, the large number of antennas at the transmitter imposes high computational burdens and high hardware overloads. In line with the above, in this paper we propose a low complexity antenna selection (AS) scheme which selects the antennas that maximize constructive interference between the users. Our analyses show that the proposed AS algorithm, in combination with a simple matched filter (MF) precoder at the transmitter, is able to achieve better performances than systems equipped with a more complex channel inversion (CI) precoder and computationally expensive AS techniques. First, we give an analytical definition of constructive and destructive interference, based on the phase of the received signals from phase-shifted-keying (PSK) modulated transmissions. Then, we introduce the proposed antenna selection algorithm, which identifies the antenna subset with the highest constructive interference, maximizing the power received by the user. In our studies, we derive the computational burden of the proposed technique with a rigorous and thorough analysis and we identify a closed form expression of the upper bound received power at the user side. In addition, we evaluate in detail the power benefits of the proposed transmission scheme by defining an efficiency metric based on the achieved throughput. The results presented in this paper prove that antenna selection and green radio concepts can be jointly used for power efficient M-MIMO, as they lead to significant power savings and complexity reductions.**

***Index Terms*—Massive MIMO, Multiuser MIMO, Antenna selection, Interference optimization**

I. Introduction

Multi-User MIMO (MU-MIMO) has experienced an increasing interest in research over the past years [1]. The MU-MIMO scenario defines a system where a base station (BS), equipped with an antenna array, communicates with a population of mobile stations (MS) or users, each equipped with a single or a multiple antenna. In the first MU-MIMO approaches, the number of antennas at the BS was equal to the population of MSs [2], proving to be a non-scalable technology. The recent emergence of massive MIMO (M-MIMO) [3], [4] systems shows that very large arrays at the BS can bring significant throughput benefits.

Manuscript received November 19, 2014; revised March 18, 2015 and June 18, 2015; accepted September 02, 2015. The associate editor coordinating the review of this manuscript and approving it for publication was Dr. Ngọc-Dũng Đào.

The authors are with Department of Electronic & Electrical Engineering - University College London, Torrington Place, London WC1E 7JE, UK.

This work was supported by the Royal Academy of Engineering, UK and the Engineering and Physical Sciences Research Council (EPSRC) project EP/M014150/1.

In Massive MIMO technology, the number of radiating elements can increase up to few hundreds, performing secure, robust and energy-efficient communications [2][1]. Arrays in M-MIMO can have many different configurations and geometries, such as cylindrical or uniform linear (ULA) arrays, and are preferably characterized by small active units [2] to respect cost and space constraints. In addition, recent works [5], [6] have investigated the possibility of exploiting transmit mutual coupling at the base station, allowing the dimensions of antenna arrays in fixed physical spaces to further increase. Massive systems are characterized by higher capacities, thanks to higher degrees of freedom, and increased radiated energy efficiency, led by beamforming gains. In addition to this, simple linear precoding techniques such as MF precoding have been proved to be optimal in a M-MIMO system [7], [8] when the number of antennas at the BS tends to infinity, because the interference between users disappears.

The use of very large arrays leads to an increased hardware complexity in terms of radio-frequency (RF) chains. In fact, each antenna element at the base station is connected to a single RF chain, characterized by amplifier, analog-to-digital converter (ADC) and mixers. These elements make RF chains generally expensive and particularly power demanding. Specifically, RF chains are accountable for 50-80% of the total transceiving power consumption [9]. As a consequence, antenna selection can be seen as an interesting approach to tackle the inherent hardware complexity of M-MIMO and, at the same time, exploit the higher degrees of freedom provided by the excess of antennas at the base station.

Antenna selection in conventional MIMO system has been a key topic of research in the past years [10], [11], showing the benefits in terms of power efficiency and performances of the use of a subset of antennas in transmission or reception [12]. In particular, the authors in [13] introduced a complexity-efficient AS algorithm that aims to maximize the spectral efficiency by minimizing the losses caused by reducing the transmitting antennas, in contrast with previous techniques based on exhaustive search [14]. The norm based AS algorithm in [15] proved the benefits of selecting the antenna subset that maximizes the channel path gains, but its approach, based on an exhaustive search over all the possible subset configurations, becomes computationally demanding for high

[1]The number of radiating elements at the base station could further increase when considering mm-wave communications. In fact, the shorter wavelengths deriving from the use of these frequencies allow the design of very high dimensional arrays in limited physical spaces. However, the high values of free space attenuation experienced at these frequencies lead to the necessity of high beamforming gains, which are strongly affected by antenna selection.

dimensional MIMO operations. The same authors showed in [16] that antenna selection can maximize the received signal-to-noise ratio (SNR) for low dimensional MIMO systems with maximal ratio combining (MRC) detection. Additionally, the algorithm in [17] optimizes the error rate at the receiver for a system that employs a maximum likelihood decoder, showing significant benefits in terms of performances at the cost of high computational complexity. Finally, [18] proved that AS algorithms performed over the eigenvalues of the channel correlation matrix can improve the error rate of a MU-MIMO system, when a small number of extra antennas is considered at the transmitter. These works, among many others, proved that AS can reduce the RF complexity at the transmitter/receiver. However, their computational costs increase together with the system size, limiting their direct applicability in multiuser M-MIMO scenarios. Toward this end, recent works are studying the energy efficiency benefits offered by antenna selection for large scale MIMO systems [19]–[21]. More specifically, the study in [22] proposes an energy efficiency approach toward antenna selection, but the energy costs caused by the algorithms are not included in the analysis. In addition, the authors in [23] analyze the effects of antenna selection with a random approach, while [24] proposes an antenna selection algorithm based on Convex Optimization for a massively distributed antenna system.

This paper studies a novel low-complexity antenna selection algorithm that exploits the benefits of constructive interference [25]–[29] in a multiuser M-MIMO scenario. In fact, the interference between the links of a MIMO system can be beneficial for the transmission and improve the performances in terms of signal detection by increasing the power of the desired signal. Since interference is data dependent, the transmitter is able to predict the co-channel interference (CCI) and can use this knowledge to influence it and benefit from it. More specifically, early works in [25], [26] focused on zeroing the destructive component of interference, defined according to the correlation between the substreams of a MIMO PSK modulated transmission. Results in [27] instead, showed that the transmitted signal can be effectively precoded in order to rotate the destructive component of interference, hence aligning the interfering transmissions to the desired signal.

The developed algorithm makes full use of the high antenna diversity offered by massive arrays and selects the subset that optimizes inter channel interference (ICI), reducing the number of RF chains required for transmission and increasing the energy efficiency of the system with a favorable trade-off between performance and complexity. The proposed technique is characterized by a reduced digital signal processing (DSP) complexity, having overall computational burdens that are even lower than the ones of a full M-MIMO system with CI or a simple MF.

Here we list the contributions of the paper:

- We introduce a novel and low-complexity antenna selection algorithm for multiuser M-MIMO scenarios based on the concept of constructive interference;
- We analytically study the computational complexity of the proposed transceiver scheme in comparison with previous approaches;
- We analytically derive the upper bound of the received signal-to-interference and noise ratio (SINR) for each user, for the proposed AS algorithm;
- We analyze the performances obtained by the proposed technique in terms of symbol error rate (SER) and a novel energy efficiency metric that combines throughput with system power requirements.

The rest of the paper is organized as follows: Section II introduces the system model used throughout this work, Section III describes the selection algorithms used in the paper, the proposed AS technique is described in Section IV and Section V presents the computational complexity study of the proposed technique in opposition to previous works. In Section VI we derive a closed form expression of the upper-bound of the received SINR for each user. Section VII is dedicated to a study of the performances obtained with the proposed system and finally, Section VIII summarizes the contributions of the paper.

Notation: We use the following notation throughout the paper. Upper case boldfaced letters identify matrices (i.e. $\mathbf{X}$), lower case boldfaced letters are used for vectors (i.e. $\mathbf{x}$), vector subindices are used to identify the rows of a matrix (i.e. $\mathbf{x}_m$ is the m-th row of $\mathbf{X}$), $tr[\cdot]$ represents the trace of a matrix, superscripts $(\cdot)^H$ and $(\cdot)^*$ stand respectively for Hermitian transpose and complex conjugate.

II. System Model

In our studies, we consider the downlink transmission of a multiuser scenario where the BS uses a very large array of N antennas to communicate with K single antenna users. The signals received by the K users can be represented through a $K \times 1$ vector $\mathbf{y}$, defined analytically as:

$$\mathbf{y} = \mathbf{H}^H \mathbf{G}\mathbf{u} + \mathbf{n} \tag{1}$$

where $\mathbf{H}$ identifies the $\mathbb{C}^{N\times K}$ channel matrix, $\mathbf{G}$ represents the $\mathbb{C}^{N\times K}$ precoding matrix, $\mathbf{u}$ stands for the $K \times 1$ vector that collects the desired symbols to transmit to each user and, finally, $\mathbf{n}$ is the $\mathbb{C}^{K\times 1}$ zero mean additive white Gaussian noise vector, i.e. $\mathbf{n} \sim \mathcal{CN}(0, \sigma^2)$. The entries $h_{n,k}$ of the channel matrix $\mathbf{H}$ represent the path gains between the n-th antenna of the BS and the k-th user, generally modeled in M-MIMO as follows [4]

$$h_{n,k} = t_{n,k}\sqrt{\beta_k} \tag{2}$$

where $t_{n,k}$ identifies the complex small scale fading experienced between the n-th antenna and the k-th user and β_k represents the real large scale fading coefficient of the k-th user. For our studies, we consider a simple single cell scenario where the channel entries are modeled as independent Rayleigh fading, i.e. $h_{n,k}$ are zero mean i.i.d. complex Gaussian variables [30].

Throughout the paper, we analyze the performances with two different linear precoding techniques: channel inversion (CI) and matched filter (MF). The choice of linear precoding techniques is supported by the results of previous works [7], [8], which proved the asymptotic optimality of matched filter in M-MIMO, in contrast with computationally more expensive non-linear techniques.

A. Channel Inversion

Channel inversion is a simple linear precoding zero forcing technique that has been extensively studied in the past [31], [32]. The precoding matrix is obtained through the following optimization problem:

$$\mathbf{F}_{CI} = \arg\min_{\mathbf{F}} \left\{ |\mathbf{H}^H \mathbf{F}\mathbf{u} - \mathbf{u}|^2 \right\} \tag{3}$$

whose solution is obtained when $\mathbf{H}^H\mathbf{F} = \mathbf{I}_K$. Hence the precoding matrix $\mathbf{G}_{CI}$ is defined as the Moore-Penrose pseudoinverse of the channel $\mathbf{H}$

$$\mathbf{G}_{CI} = \gamma_{CI}\mathbf{F}_{CI} = \gamma_{CI}\mathbf{H}(\mathbf{H}^H\mathbf{H})^{-1} \tag{4}$$

where $\gamma_{CI} = \sqrt{1/tr[(\mathbf{H}^H\mathbf{H})^{-1}]}$ is the scaling factor [5], necessary to ensure that the transmitted signal $\mathbf{x}$ respects power constraints, $E\left\{||\mathbf{x}||^2\right\} = 1$, with $E\{\cdot\}$ being the expectation operator.

B. Matched Filter

The matched filter, is a precoding techniques that aims to maximize the received SNR at the user side by solving the following optimization problem [31]

$$\mathbf{F}_{MF} = \arg\max_{\mathbf{F}} \left\{ \frac{E\left\{|\mathbf{u}^H\mathbf{y}|\right\}}{\sigma^2} \right\} \tag{5}$$

whose solution can be identified in the Hermitian of the channel matrix $\mathbf{H}$, hence leading to

$$\mathbf{G}_{MF} = \gamma_{MF}\mathbf{F}_{MF} = \gamma_{MF}\mathbf{H} \tag{6}$$

where γ_{MF} is the scaling factor for the matched filter, defined analytically as [33]

$$\gamma_{MF} = \frac{1}{\sqrt{tr[(\mathbf{H}\mathbf{H}^H)]}}. \tag{7}$$

III. Transmit Antenna Selection: Benchmark Techniques

In the following section, we describe the antenna selection techniques used throughout the paper. In order to compare the proposed transmitter scheme with the existing antenna selection techniques for multiuser MIMO found in literature, we consider a SNR maximization selection [15], [16], a capacity maximization technique [13] and a low complexity selection over the minimum eigenvalue [18]. The SNR approach has been selected because of its low computational complexity in comparison with other techniques of the literature, which is a crucial element in M-MIMO environments for the high dimensionality of the systems involved. In addition, the eigenvalue and capacity selection allow us to compare the proposed technique with near optimal AS algorithms in terms of spectral efficiency.

Algorithm 1 Capacity Maximization

Input: $\mathbf{H}$, SNR, N_s
Output: $\widetilde{\mathbf{H}}$

- $\mathbf{A} := \mathbf{H}$
- $\mathbf{B} := \left(\mathbf{I}_K + SNR \cdot \mathbf{A}^H\mathbf{A}\right)^{-1}$
- **for** $n = 1 \rightarrow N - N_s$
  - $[\delta_1, ..., \delta_{N-n}]^T = \mathbf{A}\mathbf{B}\mathbf{A}^H$
  - $\Delta_n = \arg\min\{\delta_1, ..., \delta_{N-n}\}$
  - $\mathcal{N} = \{\Delta_1, \Delta_2, ..., \Delta_n\}$
  - $\mathbf{B} := \mathbf{B} + \mathbf{B}\mathbf{a}_{\Delta_n}^H \left(SNR^{-1} - \mathbf{a}_{\Delta_n}\mathbf{B}\mathbf{a}_{\Delta_n}^H\right)^{-1} \mathbf{a}_{\Delta_n}\mathbf{B}$
  - $\mathbf{A} := [\mathbf{a}_m]_{m \notin \mathcal{N}}$
- **end**
- $\widetilde{\mathbf{H}} = [\mathbf{h}_m]_{m \notin \mathcal{N}}$

A. SNR Maximization Antenna Selection (SM)

We define as SNR Maximization (SM), the antenna selection criterion based on the channel gain. The SM approach is a simple selection criterion based on [15], [16] that aims to identify the subset of antennas characterized by the highest channel gains with a suboptimal approach. The criterion can be analytically defined as follows

$$\mathcal{M} = \arg\max_{N_s} \left\{ |\mathbf{h}_1|^2, ..., |\mathbf{h}_N|^2 \right\} \tag{8}$$

where $\max_{N_s}$ identifies the N_s highest values of the argument, $\mathcal{M}$ is the antennas index subset obtained by the selection and $N_s = |\mathcal{M}|$ is the subset size.

B. Capacity Maximization Antenna Selection (CM)

The CM algorithm was introduced by [13] and identifies the antenna subset that minimizes the capacity losses caused by a system that uses only N_s out of N antennas. We define the capacity in downlink for a multiuser system as

$$\mathcal{E} = log_2\left[\det\left(\mathbf{I}_K + SNR \cdot \mathbf{H}^H\mathbf{P}\mathbf{H}\right)\right] \tag{9}$$

where $\mathbf{I}_K$ is a $K \times K$ identity matrix and $\mathbf{P}$ is a $N \times N$ diagonal matrix whose non-null entries $p_{n,n} = 1$ represent the transmitted power assigned to each radiating element, here considered all equal and unitary. The deactivation of transmitting antennas in a multiuser MIMO system leads to losses in the maximum achievable capacity. The loss $\mathcal{E}_l$ that occurs after the l-th antenna deactivation can be described analytically [13] by the following equation

$$\begin{aligned} \mathcal{E}_l &= log_2\left[1 + SNR \cdot \mathbf{h}_l\left(\mathbf{I}_K + SNR \cdot \mathbf{H}^H\mathbf{H}\right)^{-1}\mathbf{h}_l^H\right] \\ &= log_2\left[1 + SNR \cdot \delta_l\right]. \end{aligned} \tag{10}$$

where $\delta_l = \mathbf{h}_l\left(\mathbf{I}_K + SNR \cdot \mathbf{H}^H\mathbf{H}\right)^{-1}\mathbf{h}_l^H$ is the selection metric used to minimize the loss $\mathcal{E}_l$.

The index Δ_n of the antenna to deactivate can be identified via the following criterion

$$\Delta_n = \arg\min\{\delta_1, ..., \delta_l, ...\delta_N\}. \tag{11}$$

It follows that the CM algorithm has to be applied in a recursive manner, described analytically in Algorithm 1, where $\mathcal{N}$ represents the subset of deactivated antennas.

Algorithm 2 Minimum Eigenvalue Maximization

Input: $\mathbf{H}$, N_s
Output: $\widetilde{\mathbf{H}}$

- **for** $n = 1 \rightarrow N - N_s$
  - **for** $l = 1 \rightarrow N - n$
    - $\mathbf{R}_{(l)} = \mathbf{H}_l^H \mathbf{H}_l$
    - $\lambda_{min}^l = \min \tilde{\lambda} \left\{ \mathbf{R}_{(l)} \right\}$
  - **end**
  - $\Lambda_n = \arg\max \left\{ \lambda_{min}^1, \lambda_{min}^2, ..., \lambda_{min}^{N-n} \right\}$
  - $\mathcal{N} = \{\Lambda_1, \Lambda_2, ..., \Lambda_n\}$
- **end**
- $\widetilde{\mathbf{H}} = [\mathbf{h}_m]_{m \notin \mathcal{N}}$

C. Minimum Eigenvalue Maximization Antenna Selection (MEM)

The MEM algorithm represents a low complexity application of the technique introduced by [18]. The antenna selection presented in [18] is based on an exhaustive search of the antenna subset that leads to a maximization of minimum eigenvalue

$$\lambda_{min} = \min \tilde{\lambda} \left\{ \mathbf{H}^H \mathbf{H} \right\} \tag{12}$$

where $\tilde{\lambda}$ represents the operation necessary to obtain the eigenvalues of its argument. This approach is particularly demanding for MIMO systems in terms of computational power and becomes rapidly prohibitive as the number of users and antenna elements at the BS increases. As a consequence, direct applications of [18] in M-MIMO are not viable, because of the high number of iterations they require. In order to perform a selection over the minimum eigenvalue λ_{min} we propose a decremental application of the algorithm, following the work in [34], where the number of antennas at the transmitter is gradually decreased. At each iteration, the algorithm identifies the antenna whose deactivation brings to the intermediate subset with the highest λ_{min}, as defined analytically in Algorithm 2.

IV. Proposed Constructive Interference Maximization Antenna Selection (CIM)

The proposed scheme combines a low-complexity MF and AS to optimize the constructive interference at the receiver side. For a generic MF precoder, the received signal $\mathbf{y}_0$ in a system without noise can be defined as

$$\mathbf{y}_0 = \gamma_{_{MF}} \mathbf{R} \mathbf{u} \tag{13}$$

where $\mathbf{R} = \left(\mathbf{H}^H \mathbf{H} \right)$ is the channel cross-correlation matrix. Hence, the received signal at the k-th user y_k can be defined as

$$y_k = \rho_{k,k} u_k + ICI_k \tag{14}$$

$$ICI_k = \sum_{i=1, i \neq k}^{K} \rho_{k,i} u_i \tag{15}$$

where ICI_K represents the interference experienced by the k-th user and $\rho_{k,i}$ is used to identify the the k-th element of the i-th column of $\mathbf{R}$.

Algorithm 3 Constructive Interference Maximization for BPSK

Input: $\mathbf{H}$, $\mathbf{u}$, N_s
Output: $\widetilde{\mathbf{H}}$

- **for** $n = 1 \rightarrow N$
  - $\mathbf{R}_n = \mathbf{h}_n^H \mathbf{h}_n$
  - $[\phi_1, ..., \phi_k, ..., \phi_K]^T = Re\left[\left(\mathbf{R}_n - diag\left\{ \mathbf{R}_n \right\} \right) \mathbf{u} \right] \circ \mathbf{u}$
  - $\psi_n = \min \left\{ \phi_1, ..., \phi_k, ..., \phi_K \right\}$
- **end**
- $\mathcal{M} = \arg\max_{N_s} \left\{ \psi_1, ..., \psi_n, ..., \psi_N \right\}$
- $\widetilde{\mathbf{H}} = [\mathbf{h}_m]_{m \in \mathcal{M}}$

Following the work in [25], we can easily differentiate interference as constructive and destructive when signals are modulated with a phase-shift keying approach (PSK)[2]. We first consider a binary phase shift keying (BPSK) signal, leading to the following definitions of constructive and destructive ICI sets ($\mathcal{C}$ and $\mathcal{D}$) for the k-th user

$$\mathcal{C} : \{ i | sign(u_k) = sign\left(Re\left[\rho_{k,i} u_i \right] \right) \} \tag{16}$$

$$\mathcal{D} : \{ i | sign(u_k) \neq sign\left(Re\left[\rho_{k,i} u_i \right] \right) \} \tag{17}$$

where $sign(\cdot)$ and $Re[\cdot]$ identify the sign and the real part of the argument respectively. From (16) and (17), we can identify the constructive and destructive interference components for the k-th desired symbols as

$$C_k^{ICI} = \sum_{i \in \mathcal{C}} \rho_{k,i} u_i \tag{18}$$

$$D_k^{ICI} = \sum_{i \in \mathcal{D}} \rho_{k,i} u_i. \tag{19}$$

The conditions for constructive and destructive ICI, expressed in (16) and (17), can be similarly defined for higher order PSK modulations [26].

In particular, we can describe the conditions for constructive interference, with QPSK modulation, as a bi-dimensional version of (16) and (17). In fact, interference for QPSK modulation requires both real and imaginary part of the received signal. In formulas:

$$\begin{aligned} \mathcal{C} : \{ i | \quad & sign(Re[u_k]) = sign\left(Re\left[\rho_{k,i} u_i \right] \right) \\ & \cap \, sign(Im[u_k]) = sign\left(Im\left[\rho_{k,i} u_i \right] \right) \} \end{aligned} \tag{20}$$

$$\begin{aligned} \mathcal{D} : \{ i | \quad & sign(Re[u_k]) \neq sign\left(Re\left[\rho_{k,i} u_i \right] \right) \\ & \cup \, sign(Im[u_k]) \neq sign\left(Im\left[\rho_{k,i} u_i \right] \right) \}. \end{aligned} \tag{21}$$

Note that the aforementioned conditions for $\mathcal{C}$ and $\mathcal{D}$ need to be jointly satisfied in order to have constructive or destructive interference, respectively.

[2]As previously stated, the metric used to differentiate between constructive and destructive interference introduced in [25] is based on the assumption of PSK signaling. However, a similar metric can be applied over the outer constellation points of a quadrature amplitude modulation (QAM) signal and to the whole constellation by use of adaptive decision thresholds to accommodate constructive interference.

Finally, we derive the constructive interference conditions for 8-PSK modulations through geometrical considerations [26]

$$\begin{aligned}\mathcal{C}:\{i| \quad & (\sqrt{2}-1)Re\left[\frac{\rho_{k,i}u_i}{u_k}\right] \leq Im\left[\frac{\rho_{k,i}u_i}{u_k}\right] \\ & \cap Im\left[\frac{\rho_{k,i}u_i}{u_k}\right] \leq \left[\frac{1}{(\sqrt{2}-1)}\right] Re\left[\frac{\rho_{k,i}u_i}{u_k}\right]\}.\end{aligned} \tag{22}$$

Since a definition similar to (22) for the destructive interference set $\mathcal{D}$ is complex, it can be easily identified through a simple operation between sets, as

$$\mathcal{D}:\mathcal{N}-\mathcal{C} \tag{23}$$

where $\mathcal{N}$ is used to identify the full set of interference components. As shown in (22), the conditions for constructive interference become more complex for high order PSK modulations. However, the proposed technique is mostly suitable for high interference scenarios, where current standards make use of low order modulations, as BPSK/QPSK, to guarantee acceptable error rates.

In order to exploit the constructive interference energy, we select the antenna subset that, within a channel realization, is characterized by the highest value of the minimum constructive interference. A straightforward application of the antenna selection would require to compute C_k^{ICI} for each user k and select the minimum value for each of all the possible combinations of a subset of size N_s. This simple approach becomes computationally prohibitive for systems with a high number of antennas and users, leading to $\binom{N}{N_s} = \frac{N!}{N_s!(N-N_s)!}$ possible subset combinations. The approach to antenna selection can be simplified thanks to matrix algebra, by using the property

$$\mathbf{H}^H\mathbf{H} = \sum_{i=1}^{N}\mathbf{h}_i^H\mathbf{h}_i = \sum_{i=1}^{N}\mathbf{R}_i, \tag{24}$$

where $\mathbf{R}_i$ is defined as the i-th antenna cross-correlation. A symbol by symbol control of ICI is computationally prohibitive for highly populated scenarios, because it would require to compute the condition (16) K^2-K times. In order to maintain a low computational complexity, we define a new parameter ψ_n that defines the interference related to the n-th antenna for a BPSK modulated signal

$$\begin{aligned}\psi_n &= \min\left\{Re\left[u_k\right]Re\left[\sum_{i=1,i\neq k}^{K}\rho_{k,i}^{(n)}u_i\right],\forall k\right\} \\ &= \min\left\{\phi_k^{(n)},\forall k\right\}\end{aligned} \tag{25}$$

where $\phi_k^{(n)} = Re\left[u_k\right]Re\left[\sum_{i=1,i\neq k}^{K}\rho_{k,i}^{(n)}u_i\right]$ is the decision metric for the n-th antenna and $\rho^{(n)}$ is used to identify the elements of $\mathbf{R}_n$. Hence, the algorithm computes the ψ_n for all the N available antennas, and selects the N_s antennas that correspond to the highest values. More specifically, the subset of selected antennas $\mathcal{M}$ can be defined as follows:

$$\begin{aligned}\mathcal{M} &= \arg\max_{N_s}\left\{\min\left\{Re\left[u_k\right]Re\left[\sum_{i=1,i\neq k}^{K}\rho_{k,i}^{(n)}u_i\right],\forall k\right\},\forall n\right\} \\ &= \arg\max_{N_s}\left\{\min\left\{\phi_k^{(n)},\forall k\right\},\forall n\right\}\end{aligned} \tag{26}$$

Algorithm 4 Constructive Interference Maximization for QPSK

Input: $\mathbf{H}$, $\mathbf{u}$, N_s
Output: $\widetilde{\mathbf{H}}$

- **for** $n = 1 \rightarrow N$
  - $\mathbf{R}_n = \mathbf{h}_n^H\mathbf{h}_n$
  - $\mathbf{t} = (\mathbf{R}_n - diag\left\{\mathbf{R}_n\right\})\mathbf{u}$
  - $[\phi_1,...,\phi_K]^T = Re\left[\mathbf{u}\right]\circ Re\left[\mathbf{t}\right] + Im\left[\mathbf{u}\right]\circ Im\left[\mathbf{t}\right]$
  - $\psi_n = \min\left\{\phi_1,...,\phi_k,...,\phi_K\right\}$
- **end**
- $\mathcal{M} = \arg\max_{N_s}\left\{\psi_1,...,\psi_n,...,\psi_N\right\}$
- $\widetilde{\mathbf{H}} = [\mathbf{h}_m]_{m\in\mathcal{M}}$

The selection technique is described analytically in Algorithm 3, where $\circ$ is used to identify the Hadamard product.

As previously shown, constructive interference can also be used to enhance the received SNR of higher order PSK modulated transmissions. Considering the conditions described in Eq. (20), we can define a new selection metric for QPSK modulation as

$$\begin{aligned}\phi_{k,QPSK} \quad = \quad & Re\left[(\mathbf{R}_n - diag\left\{\mathbf{R}_n\right\})\mathbf{u}\right]\circ Re\left[\mathbf{u}\right] + \\ & Im\left[(\mathbf{R}_n - diag\left\{\mathbf{R}_n\right\})\mathbf{u}\right]\circ Im\left[\mathbf{u}\right]\end{aligned} \tag{27}$$

and the selected antennas $\mathcal{M}_{QPSK}$ as

$$\mathcal{M}_{QPSK} = \arg\max_{N_s}\left\{\min\left\{\phi_{k,QPSK}^{(n)},\forall k\right\},\forall n\right\}. \tag{28}$$

The CIM selection for QPSK signaling is described analytically in Algorithm 4.

The antenna selection for QPSK preserves part of the destructive interference, because of the tightening on constructive interference conditions in (20). We propose a hybrid approach that nullifies the destructive interference components which could not be optimized by the presented antenna selection, while preserving the constructive interference benefits introduced by CIM algorithm. This is obtained through the definition of a constructive correlation matrix $\mathbf{R}_\phi$ whose entries can be analytically described as

$$\rho_\phi(n,k) = \begin{cases}\rho_{n,k} & \text{if } \rho_{n,k}\in\mathcal{C} \\ 0 & \text{if } \rho_{n,k}\notin\mathcal{C}\end{cases} \tag{29}$$

Hence, we can define the precoding matrix as [25]

$$\mathbf{G}_{HY} = \gamma_{_{HY}}\widetilde{\mathbf{H}}(\widetilde{\mathbf{H}}^H\widetilde{\mathbf{H}})^{-1}\mathbf{R}_\phi \tag{30}$$

where $\widetilde{\mathbf{H}}$ indicates the equivalent channel matrix after the antenna selection and $\gamma_{_{HY}} = \sqrt{1/tr\left[\mathbf{R}_\phi^H(\mathbf{H}\mathbf{H}^H)^{-1}\mathbf{R}_\phi\right]}$ represents the scaling factor [25].

V. System Computational Complexity

One of the effects brought by the use of hundreds of antennas in M-MIMO systems is a significant increase in computational costs, even when linear precoding techniques are involved in the transmission. In this section, we study the

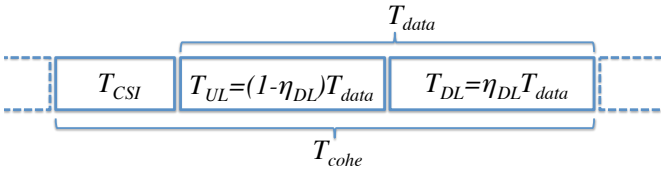

Fig. 1. Representation of T_{cohe} in a TDD system.

complexity of precoding and antenna selection techniques of all the transceiving configurations in terms of floating-point operations per second (FLOPs), following the analysis in [35], based on the costs listed in the literature [36]. In particular, we first present a thorough analysis of linear precoding techniques costs for systems that do not involve antenna selection, followed by a study of the computational burden of the schemes that involve the antenna selection techniques presented in the paper.

We consider a TDD scenario [35], [37], where the maximum number of symbols that can be transmitted when channel propagation elements in $\mathbf{H}$ are constant is defined as coherence time T_{cohe}. In frequency division duplexing (FDD) M-MIMO scenarios, the time necessary to acquire channel state information (CSI) at the transmitter is particularly relevant and significantly reduces the number of symbols $T_{data} \ll T_{cohe}$ dedicated to data transmission [37]. Thanks to our previous TDD assumption, we can exploit the reciprocity of the channel and we can define the number of slots used for CSI acquisition T_{CSI} via direct proportionality to the number of users K, instead of the array dimension at the base station N. This leads to the following relationship

$$T_{data} = T_{cohe} - \mu K \tag{31}$$

where $\mu \geq 1$ is a parameter that defines the number of pilot symbols used for CSI per user. In addition, when considering a TDD protocol system, only a fraction η_{DL} of T_{data} is used for downlink transmission, defining the amount of data symbols that can be transmitted to the users during a single coherence time as

$$T_{DL} = \eta_{DL} \left(T_{cohe} - T_{CSI}\right) \tag{32}$$

and the amount of data symbols that can be transmitted from the users to the BS as

$$T_{UL} = \left(1 - \eta_{DL}\right) \left(T_{cohe} - T_{CSI}\right). \tag{33}$$

The relationship between T_{cohe} and T_{DL} is visually represented in Fig.1. We list the associated costs for each of the AS schemes discussed in Table I.

A. Precoding

The dominant costs of CI precoding can be identified in the following steps:

- Compute the correlation matrix $\mathbf{R} = \mathbf{H}^H\mathbf{H}$
- Compute the inverse of $\mathbf{R}$
- Multiply $\mathbf{R}^{-1}$ by $\mathbf{H}$
- Apply the precoding matrix $\mathbf{G}_{CI}$ to the data $\mathbf{u}$

The number of operations necessary for each step of the precoding procedure depends on the matrix size [36]. Matrix inversion is particularly expensive, as its computational complexity grows exponentially with the size $\frac{8}{3}K^3$, but it is computed only once per coherence time. At the same time, the precoding procedure in M-MIMO becomes significant for the complexity count. In fact, due to the size of the matrices involved, the costs of the precoding $\mathbf{G}_{CI}\mathbf{u}$ become particularly relevant in the final computational count.

In opposition to channel inversion, MF precoding is based only on the computation of the Hermitian transpose of the channel matrix and its application to $\mathbf{u}$. As a consequence, main costs of MF reside in the application of precoding to the data signal vector $\mathbf{u}$.

B. Antenna Selection

1) SM Antenna Selection: The SM algorithm has low complexity, since it is characterized by two operations only: the computation of the antenna path gains, as the diagonal of the correlation matrix $\mathbf{R} = \mathbf{H}\mathbf{H}^H$, and the identification of the N_s highest values.

2) CM Antenna Selection: The CM algorithm has a very high complexity as its key operations are particularly demanding. In particular, we need to: compute the matrix $\mathbf{B} = \left(\mathbf{I}_K + SNR \cdot \mathbf{H}^H\mathbf{H}\right)^{-1}$, select the minimum value of δ_n and, finally, update the matrix $\mathbf{B}$. Main costs reside in the iterative nature of this approach, as it leads to the need to repeat each of these steps $N - N_s$ times. Since the sizes of the channel matrix at intermediate stages $\bar{\mathbf{H}}$ change at each iteration of CM, the computational costs of this technique require the use of a summation, whose elements are a function of the iteration number and N_s.

3) MEM Antenna Selection: The MEM algorithm is affected by the highest computational costs as it requires to compute the eigenvalues of intermediate stages correlation matrices several times within a single iteration. More specifically, MEM is characterized by $N - N_s$ iterations, each one characterized by the necessity to compute $N - l$ times the eigenvalues of $\bar{\mathbf{H}}^H\bar{\mathbf{H}}$, where l is the iteration step. In order to evaluate the computational burdens of MEM, we consider a tridiagonal QR algorithm for the computation of the eigenvalues, with the assumption that $\mathbf{R}$ has been previously reduced to a tridiagonal form [38].

The costs of this approach are particularly high and prohibitive for M-MIMO.

4) Proposed CIM Antenna Selection: The computational costs for the CIM algorithm can be identified mainly in the following steps:

- Compute the antenna cross-correlation matrix $\mathbf{R}_n = \mathbf{h}_n^H\mathbf{h}_n$
- Compute the decisional parameter ψ_n
- Identify maximum values of ψ_n

A detailed study of the computational burden of the proposed transceiving schemes, within a single T_{cohe}, is reported in Table I, along with the total complexity of each of the AS schemes.

Full System with CI		**Full System with MF**	
$\mathbf{R}$	$K(2K+1)(4N-1)$	$\mathbf{G}_{MF}$	KN
$\mathbf{R}^{-1}$	$\frac{8}{3}K^3$	$\mathbf{G}_{MF}\mathbf{u}$	$T_{DL}2N(4K-1)$
$\mathbf{G}_{CI}$	$4KN(4K-1)$	–	–
$\mathbf{G}_{CI}\mathbf{u}$	$T_{DL}2N(4K-1)$	–	–
Total	$2(K^2+K)(4N-1)+\frac{8}{3}K^3+$ $4KN(4K-1)+T_{DL}2N(4K-1)$	**Total**	$KN+T_{DL}2N(4K-1)$
SM Ant. Sel. with CI		**CM Ant. Sel. with CI**	
$\mathbf{H}\mathbf{H}^H$	$N(2N+1)(4K-1)$	$\mathbf{B}$	$K(2K+1)(4N-1)+2K+\frac{8}{3}K^3$
$\widetilde{\mathbf{H}}$	N	$\mathbf{A}\mathbf{B}\mathbf{A}^H$	$\sum_{l=1}^{N-N_s}[4(N-l)K(4K-1)+(N-l)[2(N-l)+1](4K-1)]$
$\mathbf{R}$	$K(2K+1)(4N_s-1)$	$\mathbf{B}$	$\sum_{l=1}^{N-N_s}[2K(4K-1)+(4K-1)+4K(4K-1)+K^2]$
$\mathbf{R}^{-1}$	$\frac{8}{3}K^3$	$\widetilde{\mathbf{H}}$	$\sum_{l=1}^{N-N_s}(N-l)$
$\mathbf{G}_{CI}$	$4KN_s(4K-1)$	$\mathbf{R}$	$K(2K+1)(4N_s-1)$
$\mathbf{G}_{CI}\mathbf{u}$	$T_{DL}2N_s(4K-1)$	$\mathbf{R}^{-1}$	$\frac{8}{3}K^3$
–	–	$\mathbf{G}_{CI}$	$4KN_s(4K-1)$
–	–	$\mathbf{G}_{CI}\mathbf{u}$	$T_{DL}2N_s(4K-1)$
Total	$(4K-1)(2N^2+N+4KN_s+2N_sT_{DL})+$ $(2K^2+K)(4N_s-1)+\frac{8}{3}K^3+N$	**Total**	$\sum_{l=1}^{N-N_s}[4(N-l)K(4K-1)+(N-l)[2(N-l)+1](4K-1)]+\frac{16}{3}K^3$ $\sum_{l=1}^{N-N_s}[2K(4K-1)+(4K-1)+4K(4K-1)+K^2+(N-l)]+2K$ $(2K^2+K)(4N+4N_s-2)+(4K-1)(4KN_s+2N_sT_{DL})$
CIM Ant. Sel. with MF		**MEM Ant. Sel. with CI**	
$\mathbf{R}_n$	$NK(2K+1)$	$\mathbf{R}$	$\sum_{l=1}^{N-N_s}K(2K+1)(4(N-l)-1)$
ψ_n	BPSK: $T_{DL}NK(2K-3)$	λ_{min}	$\sum_{l=1}^{N-N_s}[K+(N-l)(\frac{64}{3}K^3+4K^2)]$
	QPSK: $2T_{DL}NK(2K-3)$	$\widetilde{\mathbf{H}}$	$\sum_{l=1}^{N-N_s}K$
$\widetilde{\mathbf{H}}$	$T_{DL}N$	$\mathbf{R}$	$K(2K+1)(4N_s-1)$
$\mathbf{G}_{MF}\mathbf{u}$	$T_{DL}2N_s(4K-1)$	$\mathbf{R}^{-1}$	$\frac{8}{3}K^3$
–	–	$\mathbf{G}_{CI}$	$4KN_s(4K-1)$
–	–	$\mathbf{G}_{CI}\mathbf{u}$	$T_{DL}2N_s(4K-1)$
Total	BPSK: $NK(2K+1)+T_{DL}NK(2K-3)+$ $T_{DL}N+T_{DL}2N_s(4K-1)$	**Total**	$\sum_{l=1}^{N-N_s}[K(2K+1)(4(N-l)-1)+2K+(N-l)(\frac{64}{3}K^3+4K^2)]+$ $(2K^2+K)(4N_s-1)+\frac{8}{3}K^3+(4K-1)(4KN_s+2N_sT_{DL})$

TABLE I
COMPUTATIONAL COSTS OF DIFFERENT SCHEMES IN FLOPS

We omit from Table I the computational studies for the MF precoding over SM, CEM and MEM selection for the sake of brevity, since they can be easily obtained by substituting the $\mathbf{R} \rightarrow \mathbf{G}_{CI}\mathbf{u}$ steps with the $\mathbf{G}_{MF}\mathbf{u}$ step of the proposed scheme.

C. Transceiver Computational Costs Analysis

From Table I we can see that computational costs for linear precoding in a classical MIMO system would reside mostly in the identification of the matrix $\mathbf{G}$. In fact, costs for the application of data precoding in classic multiuser MIMO are less relevant because of the reduced sizes of the system. This is not true in M-MIMO, where the number of antennas is much larger than the number of users, leading to computational costs for precoding application that are directly proportional to N. This shows additional benefits of the antenna selection approach, because costs for precoding are strongly reduced. At the same time, the proposed antenna selection is affected by the necessity to repeat the algorithm for each T_{DL} because it is data dependent. Nonetheless, the higher costs of data dependent antenna selection over classical M-MIMO are mitigated by the higher T_{CSI} that characterizes

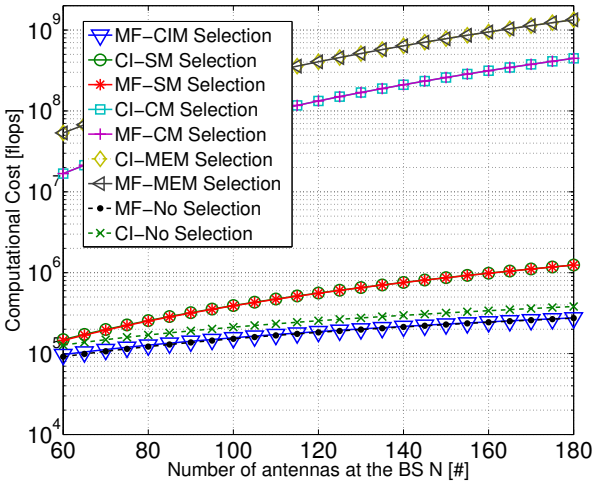

Fig. 2. Computational costs as a function of the number of antennas at the transmitter N for a BPSK modulated system with $K = 5$, $N_s = K$.

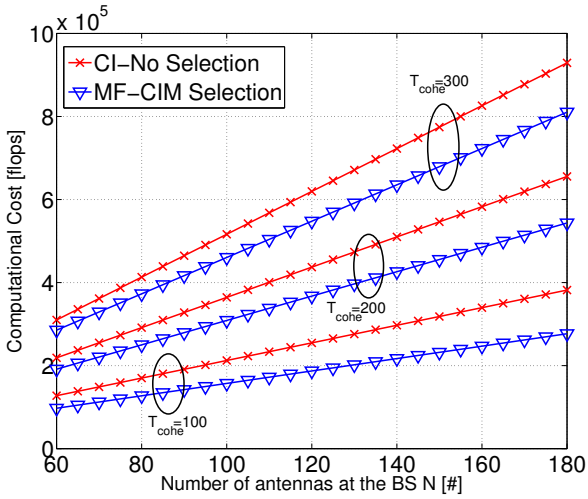

Fig. 3. Computational costs as a function of T_{cohe} for a BPSK modulated system with $K = 5$, $N_s = K$.

such systems. It is important to stress that the values shown in Table I are computed for a single coherence time, while considering the renew frequency of data dependent operations. In fact, since precoding and the proposed antenna selection have to be repeated at a symbol rate, they are characterized by a T_{DL} factor. On the other hand, the costs of classical antenna selection algorithms are considered only once per coherence time, as they compute costly metrics that are dependent on the channel realization. Consequently, they are characterized by high and nearly prohibitive computational costs, as shown in Table I.

The selection metric of the proposed algorithm changes according to the constellation order used at the transmitter, leading to different complexities, as presented in Table I. Nevertheless, as shown in Algorithm 4, we can note that the difference between the BPSK and QPSK metric is identified only in the need to compute the interference metric for both the real and the imaginary part. In addition, the algebraic property in (24) is independent from the constellation used and its cost represents an important component of the global burden of the algorithm, significantly reducing the differences between the two cases.

The effects described can be observed in Fig. 2, which shows the computational costs in FLOPs as a function of the number of antennas at the BS N, when the number of users is fixed to a specific value of K. In particular, Fig. 2 represents a fast fading scenario, i.e. T_{cohe} is shorter than a frame, with $K = 5$ users, subset size equal to the number of users $N_s = 5$ when TDD is characterized by the parameters: $T_{cohe} = 100$, $\mu = 2$ and $\eta_{DL} = 50\%$. The values used correspond to a coherence time $t_{cohe} \approx 7ms$ when considering current LTE standards for frame time $t_f = 10ms$ and symbol time $t_s = 71.4\mu s$ [4] with a single carrier transmission scheme. This assumption is not uncommon in the study of energy efficient systems, as recent works over large-scale MIMO systems [39] showed the power efficiency benefits of single-carrier transmission schemes. More specifically, [39] shows that multi-carrier OFDM modulation has a very high peak-to-average ratio, which requires the RF power amplifiers to work within an operating regime where they have low efficiency. Toward this end, the use of constant envelope precoding [40] for massive MIMO system has further showed the energy efficiency benefits of single carrier communications. In fact, as shown in [40], single carrier communications with constant envelope precoding at the transmitter allow the use of power efficient/non-linear RF components. This can be achieved by transmitting, from each antenna, signals whose amplitude is constant and independent from the channel realization. From Fig.2, we can see that previous selection techniques are characterized by high costs, due to the size of the system, leading to near overlapping curves for CI and MF. It is interesting to notice that the proposed technique has always lower costs than all the other approaches and that the difference in costs increases as the number of antennas at the BS grows.

Note that the computational costs presented in Fig.2 represent the overall FLOP count required by the systems described in the legend, including both the precoding costs and the antenna selection costs, where applicable. Simple massive MIMO approaches, CI - No selection and MF - No selection in the legend, are characterized only by channel inversion and matched filter precoding costs respectively, as they do not involve AS algorithms. On the other hand, the computational burden for antenna selection systems include both the precoding and the selection algorithm. In fact, antenna selection systems are identified in the legend according to the following notation: the first acronym for the precoding technique considered, while the latter represents the antenna selection algorithm.

Given the data dependent/interference based nature of CIM selection, its performances in terms of computational costs are affected by the length of T_{cohe}. As we would expect, computational costs increase as the number of transmitted symbols per coherence time becomes larger, but with a lower ratio than the classical MIMO approach with CI. This effect is

well described in Fig. 3, which shows the computational costs for different values of T_{cohe} for both approaches. In this figure we only show the CIM selection and the full system with CI, as results in Fig.2 show that AS algorithms of the literature experience computational burdens that are one or more orders of magnitude higher than the proposed technique.

Note that the proposed antenna selection algorithm requires a fast, symbol rate, RF switching. Due to the criticality of this element, it is important for the RF switching to be performed with low insertion losses. Toward this end, recent developments in hardware design show that GaN MMIC based switches by TriQuint [41] can achieve switching speeds on the order of ns, while offering promising performances in terms of insertion losses. In a similar manner, solid-state RF switches represent a widely used technology in modern communication systems and are able to provide switching speed inferior to $1\mu s$ [42].

In addition, it is important to state that fast symbol-rate RF switching schemes require time and bandwidth limited pulses [43] to tackle possible spectral regrowth. This cannot be realized through conventional shaping filters, such as the raised-cosine, as they are bandwidth limited and time unlimited. The design of time-limited orthogonal shaping filters was first introduced for Ultra Wide Band (UWB) systems [44]–[46], showing that it is possible to achieve pulses which are limited in time and in frequency. It is important to stress that the algorithms proposed in [44]–[46] are not UWB-dependent, as they can be tuned to respect desired time and spectral constraints, as for the proposed scheme. More specifically, the authors in [44] present a pulse shaping methodology based on the Hermite functions, while [45] presents an algorithm based on the numerical solution of the convolution between pulse and filter responses. Finally, the study in [46] presents a convex optimization metric for a DSP based pulse shaping. In addition to these works, the recent study in [43] presents a thorough analysis of the performances of different time-limited shaping filters and applies the design to a multi-antenna system that employs symbol rate RF switching.

These critical advances have fuelled the interest over single RF-chains techniques [47], which require symbol rate switching, as for Spatial Modulation MIMO (SM-MIMO)[3] [48], Space Shift Keying (SSK)[4] [43] and electronically steerable parasitic array (ESPAR)[5] communications [49]. These techniques have been successfully implemented in real systems, in [50] for SM-MIMO and [51] for ESPAR, proving how transmission schemes with similar requirements can offer increased values of energy efficiency in modern communication systems.

[3]In Spatial Modulation MIMO, a single RF chain and an antenna array are used to simultaneously transmit multiple symbols. The RF chain switches among the antennas at symbol rate, in order to modulate the information symbols over a PSK/QAM symbol and over the antenna chosen for transmission.

[4]In SSK transmission, the information bits are mapped over the index of a single radiating transmit antenna. The system switches at a symbol rate between the available antennas according to the data to be transmitted, while all the other antennas radiate no power.

[5]Over ESPAR MIMO communications, it is possible to transmit multiple streams over a single RF chain by adaptively exploiting the beam pattern characteristics of the arrays involved at the transmitter side. In fact, while the ESPAR antenna explicitly transmits a PSK/QAM symbol, additional symbols are analogically modulated by the antenna pattern, which is modified by exploiting the mutual coupling.

VI. Performance Analysis of CIM AS with MF precoding

In order to study the performances achieved by the proposed technique, we derive the upper bound of the average SINR for a single user. Following equation (13) we can generalize the received signal for the k-th user with the proposed technique as

$$y_k = \gamma_{MF}\mathbf{h}_{(k)}^H\mathbf{g}_{(k)}u_k + n_k \tag{34}$$

where $\mathbf{h}_{(k)}$ and $\mathbf{g}_{(k)}$ are used to identify the k-th column of the matrix $\mathbf{H}$ and $\mathbf{G}$ respectively and n_k is the k-th entry of the noise vector $\mathbf{n}$. We can generalize equation (34) by combining the informations in (14) with (18) and (19), leading to the following definition of received signal

$$y_k = \gamma_{MF}|\rho_{k,k}|u_k + \gamma_{MF}\sum_{i\in\mathcal{C}}|\rho_{k,i}|u_i + \gamma_{MF}\sum_{i\in\mathcal{D}}|\rho_{k,i}|u_i + n_k. \tag{35}$$

Following [25], we can define the received signal-to-interference and noise ratio (SINR) for the k-th user as

$$\xi_k = \frac{\gamma_{MF}^2|\rho_{k,k}|^2 + \gamma_{MF}^2\left(\sum_{i\in\mathcal{C}}|\rho_{k,i}|\right)^2}{\sigma^2 + \gamma_{MF}^2\left(\sum_{i\in\mathcal{D}}|\rho_{k,i}|\right)^2}. \tag{36}$$

where the constructive interference that contributes to the signal power appears at the numerator of the expression and the destructive component of the interference is added to σ^2 at the denominator, since it can be interpreted as an additional source of noise.

The received SINR is upper bounded by the condition where $D_k^{ICI} = 0$ with an optimal CIM antenna selection at the transmitter. Accordingly, an SNR upper bound can be derived as

$$\xi_k = \frac{\gamma_{MF}^2|\rho_{k,k}|^2 + \gamma_{MF}^2\left(\sum_{i\in\mathcal{C}}|\rho_{k,i}|\right)^2}{\sigma^2} \tag{37}$$

which can be seen as a generalized form of SNR, as the interference is a constructive parameter. Since we are interested in the average value of the SINR, we can apply the expectation over equation (37), leading to

$$\widetilde{\xi_k} = \frac{E\left\{\gamma_{MF}^2\left(\sum_{i=1}^{K}|\rho_{k,i}|\right)^2\right\}}{\sigma^2} = \frac{E\left\{\gamma_{MF}^2\right\}E\left\{\left(\sum_{i=1}^{K}|\rho_{k,i}|\right)^2\right\}}{\sigma^2}. \tag{38}$$

In this equation we consider γ_{MF} to be data independent, even though the conditions used to perform the antenna selection do not support this assumption. This simplification is often performed and necessary to simplify a closed form definition of $\widetilde{\xi_k}$.

In order to derive the expected value of the received SINR $\widetilde{\xi_k}$, we need to identify the statistical properties of the correlation matrix $\mathbf{R} = \mathbf{H}^H\mathbf{H}$ and its entries $\rho_{k,i}$. In an independent Rayleigh fading scenario where the entries of $\mathbf{H}$ are modelled as i.i.d Gaussian variables, the correlation

matrix $\mathbf{R}$ is known to be a Wishart matrix, characterized by the following distribution function [52]

$$f_{\mathbf{R}}(\mathbf{A}) = \frac{\pi^{-K(K-1)/2} \det \mathbf{A}^{n-K}}{\det \mathbf{\Sigma}^n \prod_{i=1}^{K}(n-i)!} e^{-Tr[\mathbf{\Sigma}^{-1}\mathbf{A}]} \quad (39)$$

where the matrix $\mathbf{\Sigma}$ is the covariance matrix of the correlation matrix $\mathbf{R}$.

We can define the absolute value of the entries $\rho_{k,i}$ of the correlation matrix, related to the k-th user, as [53]

$$|\rho_{k,i}| = \sqrt{\left[\sum_{j=1}^{N_s} h^R_{k,j}h^R_{i,j} + h^I_{k,j}h^I_{i,j}\right]^2 + \left[\sum_{j=1}^{N_s} h^I_{k,j}h^R_{i,j} - h^R_{k,j}h^I_{i,j}\right]^2} \quad (40)$$

where h^R and h^I are used to identify respectively the real and imaginary part of h. Thanks to the assumption of independent Rayleigh fading propagation, for $h^R_{k,j} \sim \mathcal{CN}(0, 1/2)$ we have

$$E\left\{\sum_{j=1}^{N_s} h^R_{k,j}h^R_{i,j} + h^I_{k,j}h^I_{i,j}\right\} = 0, \forall j \in \{1, .., N_s\} \quad (41)$$

$$var\left\{\sum_{j=1}^{N_s} h^R_{k,j}h^R_{i,j} + h^I_{k,j}h^I_{i,j}\right\} = \frac{1}{2}, \forall j \in \{1, .., N_s\} \quad (42)$$

where $var\{\cdot\}$ is used to identify the variance of the argument. These equations can be derived from $E\left\{h^R_{k,j}h^R_{i,j}\right\} = 0$ and $var\left\{h^R_{k,j}h^R_{i,j}\right\} = 1/4$, thanks to the linearity of $E\{\cdot\}$ and the uncorrelation of the entries of $\mathbf{H}$. Hence the variables $|\rho_{k,i}|$ can be distinguished between [53]:

- Rayleigh variables when $k \neq i$ with $E\{|\rho_{k,i}|\} = \frac{\sqrt{K\pi}}{2}$ and $E\left\{|\rho_{k,i}|^2\right\} = K$
- χ-squared variables when $k = i$ with $E\{|\rho_{k,i}|\} = K$ and $E\left\{|\rho_{k,i}|^2\right\} = K(K+1)$.

In order to complete the study of the upper bound received SINR of the proposed technique we need to identify the expected value of the scaling factor $E\left\{\gamma^2_{MF}\right\}$. Following (7) we have

$$E\left\{\gamma^2_{MF}\right\} = E\left\{tr\left[\mathbf{H}^H\mathbf{H}\right]^{-1}\right\}. \quad (43)$$

As previously stated, the statistical properties of the matrix $\mathbf{H}^H\mathbf{H}$ lead to [52]

$$E\left\{\gamma^2_{MF}\right\} = \frac{1}{N_sK}. \quad (44)$$

Hence, we can evaluate the upper bound of the received SINR for the k-th user as

$$\widetilde{\xi_k} = \frac{E\left\{\left(\sum_{i=1}^{K}|\rho_{k,i}|^2\right)\right\} + E\left\{\left(\sum_{j\neq i}|\rho_{k,i}||\rho_{k,j}|\right)\right\}}{N_sK\sigma^2} \quad (45)$$

The first and second term on the numerator of (45) can be rearranged in order to exploit the statistical properties listed above. In particular, for the first term we have:

$$E\left\{|\rho_{k,k}|^2 + \sum_{i\neq k}|\rho_{k,i}|^2\right\} = K(K+1) + (K-1)K \quad (46)$$

and for the second term

$$E\left\{\sum_{j\neq k}|\rho_{k,k}||\rho_{k,j}| + \sum_{j\neq i, i\neq k}|\rho_{k,i}||\rho_{k,j}|\right\} = \quad (47)$$

$$2(K-1)K\frac{\sqrt{K\pi}}{2} + (K-2)(K-1)\frac{K\pi}{4}$$

which is derived thanks to the independence of the random variables.

Hence, the equation (45) can be evaluated analytically as

$$\widetilde{\xi_k} = \frac{K(K+1) + K(K-1)(1+\sqrt{K\pi} + (K-2)\pi/4)}{N_sK\sigma^2} \quad (48)$$

A. Symbol Error probability

The previous analysis of the received SINR can be used to derive a lower bound for the symbol error probability. In fact, the symbol error probability in a M-PSK modulation is a function of the received SINR, as expressed in the following equation [27]:

$$P_\epsilon = \left(\frac{M-1}{M}\right)\left\{1 - \left(\frac{l\cdot M}{M\pi - \pi}\right)\sqrt{\frac{\sin^2\left(\frac{\pi}{M}\right)\cdot l}{1 + \widetilde{\xi}\sin^2\left(\frac{\pi}{M}\right)}}\right\} \quad (49)$$

where

$$l = \frac{\pi}{2} + \tan^{-1}\left\{\cot\left(\frac{\pi}{M}\right)\sqrt{\frac{\sin^2\left(\frac{\pi}{M}\right)\cdot l}{1 + \widetilde{\xi}\sin^2\left(\frac{\pi}{M}\right)}}\right\}. \quad (50)$$

Hence the symbol error probability for a PSK modulation can be easily computed by substituting in (49) the correct order modulation for M and the final received SINR derived in (48).

VII. Results

We evaluate the performances obtained by the proposed antenna selection technique through Monte Carlo simulations over 50000 channel realizations. We consider a single cell downlink scenario with perfect channel state information at the transmitter side, where the BS is equipped with an antenna array of $N = 100$ elements and communicates with $K = 5$ single antenna mobile users. Since we assume a single cell downlink transmission scenario where $N \gg K$ [30], we choose a subset size N_s equal to the number of users K. In our simulations we use both BPSK and QPSK modulations.

All the schemes described in the figures are characterized by a combination of precoding and antenna selection at the transmitter, with the exception of simple massive MIMO approaches used as performance references. Legends have been conventionally defined to first declare the precoding used: CI and MF for channel inversion and matched filter precoding respectively and HY to identify the hybrid approach for QPSK modulations. Finally, selection techniques are identified as follows: No AS when the BS uses all the available antennas (i.e. to identify the classical massive MIMO approaches), CIM to identify the proposed selection technique, SM when the subset is defined according to the SNR maximization criterion,

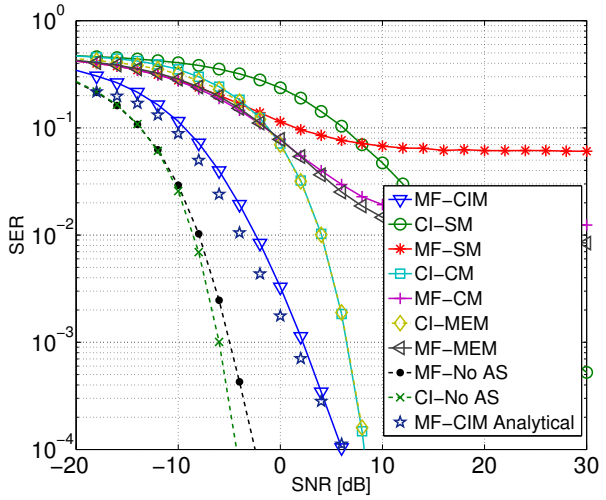

Fig. 4. SER as a function of the transmitted SNR for BPSK modulation when $N = 100$, $K = 5$ and $N_s = 5$.

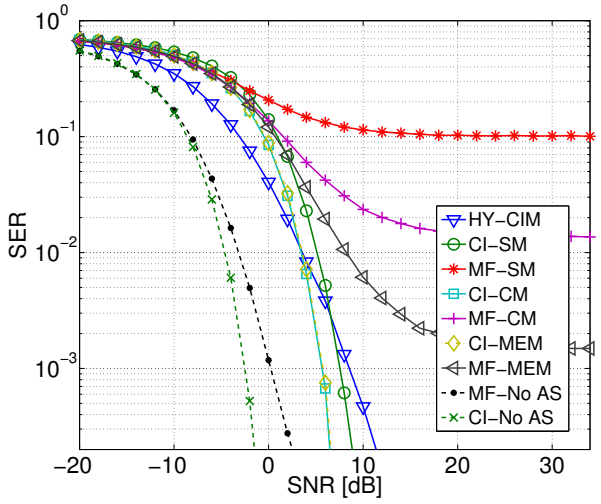

Fig. 5. SER as a function of the transmitted SNR for QPSK modulation when $N = 100$, $K = 5$ and $N_s = 10$.

CM for the capacity maximization and MEM for the minimum eigenvalue maximization selection.

Fig.4 and Fig. 5 show the symbol error rate (SER) performances as a function of the $SNR = 1/\sigma^2$ for all the configurations described, with BPSK and QPSK signaling respectively. Performances in terms of SER for both cases are higher when no antenna selection at the transmitter is involved, but they are achieved thanks to a higher hardware complexity, as previously shown. All previous antenna selection techniques with MF are characterized by strong losses in performances when N_s equals the number of users.

It is interesting to notice how in Fig.4, SM selection is characterized by strong losses even with CI precoding at the transmitter. Always in Fig.4, we can see that MEM and CM approaches with CI achieve good performances as the SNR grows, but at the expenses of high computational costs, nearly prohibitive for practical systems. On the other hand, the proposed scheme, CIM with MF, shows only minor losses in performances when compared to the full system with both CI and MF, while using only K of the N antennas available at the transmitter.

Fig.5 shows the performances of the proposed AS algorithm for a QPSK modulated scenario when the antenna subset $N_s = 10$ and $K = 5$. The performances achieved by the proposed scheme for QPSK are identified by the curve that corresponds to HY-CIM in the legend. As we can see, the proposed scheme follows similar performances to the previous and prohibitive antenna selection techniques of the literature, showing a positive trade-off between complexity and performance. It is pivotal to highlight that the showed performances for HY-CIM are achieved with significantly lower computational costs than CM or MEM, for both MF and CI cases. In addition, we can see that previous antenna selection systems that employ MF are affected by error floors. This behavior, distinctive for matched filter precoding and here kept for the sake of completeness, is caused by the inability of previous antenna selection techniques to optimize the destructive effect of interference.

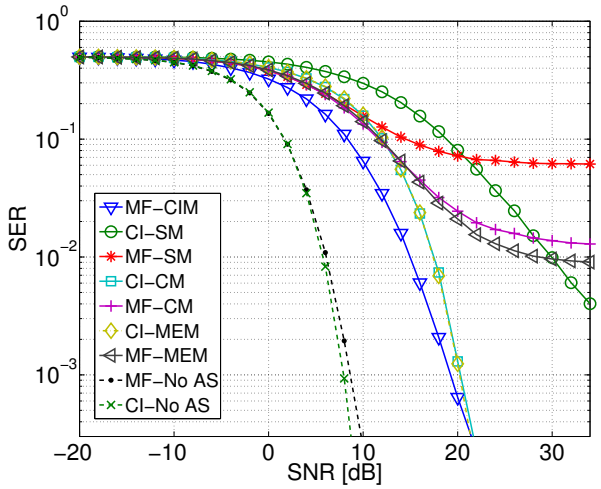

Fig. 6. SER as a function of the transmitted SNR for BPSK modulation when $N = 100$, $K = 5$ and $N_s = 5$ with imperfect CSI at the transmitter $\alpha = 10$.

In Fig.6 we further characterize the proposed scheme when imperfect CSI is considered at the base station. During antenna selection and precoding, we consider the BS to be aware of an estimated channel matrix, defined analytically as follows [54]

$$\widehat{\mathbf{H}} = \mathbf{H} + \mathbf{E} \tag{51}$$

where $\mathbf{E} \sim \mathcal{CN}(0, \beta)$ is the error matrix, statistically independent from $\mathbf{H}$, and $\beta = \frac{\alpha}{SNR} = \alpha \cdot \sigma^2$ is the variance of the estimation error for a TDD system, with α being an inverse proportionality coefficient [54]. Fig.6 shows that for a system with $\alpha = 10$, the performances of the proposed technique are affected by the errors in the channel estimation. However, it is fundamental to highlight how the performance trend of the proposed scheme follows the one of a system when perfect CSI is available at the transmitter.

In order to better illustrate the benefits brought by the proposed scheme and the performance-complexity trade-off,

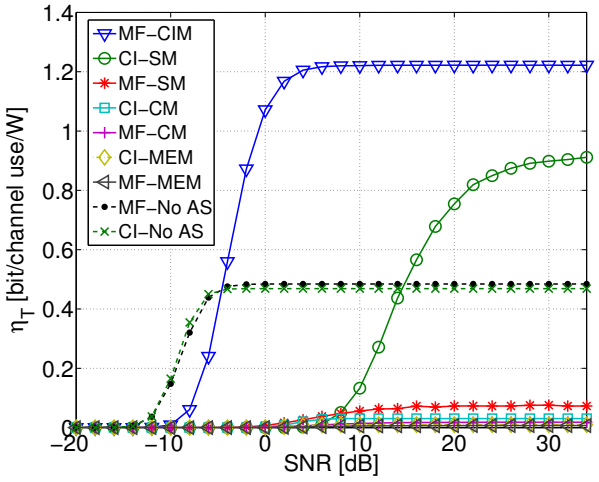

Fig. 7. Power efficiency over throughput as a function of the transmitted SNR for BPSK modulation when $N = 100$, $K = 5$ and $N_s = 5$.

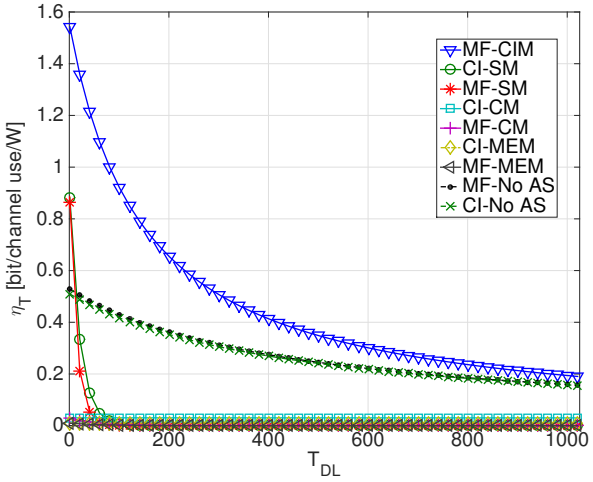

Fig. 8. Power efficiency over throughput as a function of the transmitted symbols T_{DL} when $SNR = 10dB$, $N = 100$ and $K = 5$.

we introduce a parameter which combines SER with the power requirements at the transmitter. We define the power efficiency over throughput η_T as follows [55]

$$\eta_T = \frac{T}{P_{amp} + N_s \cdot P_{RF} + N_{ops} \cdot P_{fpga}} \tag{52}$$

where $T = (1 - BLER) \cdot m \cdot K$ is the throughput, $BLER$ is the block error rate, $m = 1$ for BPSK and $m = 2$ for QPSK, P_{amp} $[W]$ is the power required by the amplifier, P_{RF} $[W]$ is the power consumption of a single RF chain, characterized by digital-analog converter, mixer and filter, $N_{ops}[KFLOPs]$ identifies the complexity burden of the analyzed technique in terms of 10^3 floating point operations, based on the complexity values computed in Table I, and P_{fpga} $[W/KFLOPs]$ is the power consumption per operation of the field-programmable gate array (FPGA). We model the values necessary to compute (52) from practical systems [55], [56], where $P_{amp} = P_t/\nu$ is defined as the power required by an amplifier with $\nu = 0.35$ efficiency in order to have a transmitted power $P_t = 30dBm$, $P_{RF} = 65.9mW$ and $P_{fpga} = 5.76mW/KFLOPs$.

Fig.7 describes the results in terms of power efficiency over throughput for a BPSK scenario, showing that the proposed approach is characterized by higher values of efficiency than all the other techniques, including the system without selection for both CI and MF precoding. The higher power efficiency of MF-CIM is supported by the lower hardware complexity it requires, with reduced values of power at the denominator in (52), in order to achieve similar performances. In addition to the computational savings, the proposed approach with CIM antenna selection is able to achieve the showed performances with only 5% of the RF power required at the transmitter by the full system, when no antenna selection is involved. On the other hand, we can see that previous AS algorithms are characterized by very low power efficiency because of the high computational burdens they are affected by. In fact, the increased power consumed by the FPGA is high enough to overcome the RF power savings.

Figure 8 presents the power efficiency as a function of the number of single carrier symbols during the downlink T_{DL} when $SNR = 10dB$. As we can see from Fig.8, the proposed technique MF-CIM maintains higher performances than the other approaches for increasing values of T_{DL}. The performance gap between MF-CIM and the systems without antenna selection reduces as T_{DL} grows, however it is important to note that the proposed scheme keeps outperforming the classical MIMO approach until $T_{DL} \approx 1000$. These values of T_{DL} correspond to an OFDM modulated scenario with coherence time of 10 OFDM symbols with 256 sub-carriers.[6]

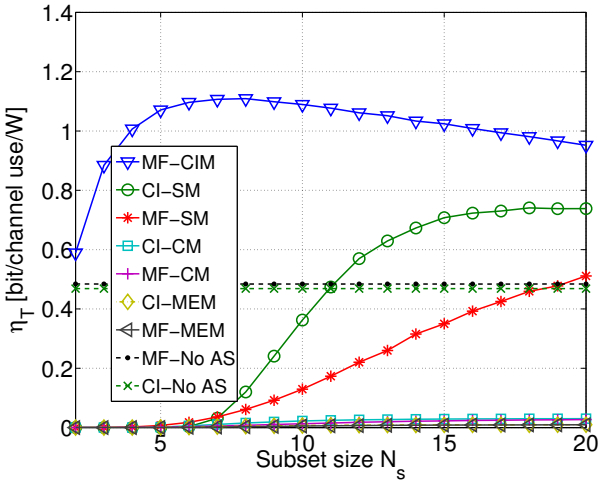

Fig. 9. Power efficiency over throughput as a function of the subset size N_s when $SNR = 0dB$, $N = 100$ and $K = 5$.

In order to identify the subset size that optimizes the trade-off between complexity and performances, we evaluate the power efficiency as a function of N_s. As shown in Fig.9,

[6]In fact, if we consider a $T_{cohe} = 10$ OFDM symbols and $T_{CSI} = 2$ OFDM symbols, we would have a $T_{DL} = 4$ OFDM symbols ($T_{DL} = 4*256$ sub-carriers roughly corresponds to $T_{DL} = 1000$ symbols). These values are often used when analyzing massive MIMO systems, as in the work by [37] where a coherence time with $T_{cohe} = 7$ OFDM symbols is considered.

$N_s = K$ proves to be a near optimal choice, as the CIM-MF curve presents a peak around $N_s = 6/7$. Since the difference in terms of efficiency between $N_s = K = 5$ and $N_s = 7$ is negligible, for our studies, we decided to consider the simple case where one transmit antenna is assigned per each user. In addition, it is interesting to notice how the power efficiency of the full system is higher than all the previous antenna selection algorithms presented in this paper, with the exception of SM, independently from the choice of N_s. We can once more justify this phenomenon by the high computational costs of MEM and CM algorithms, whose power consumptions overcome the savings introduced by the use of a limited set of RF chains. To this end, Fig. 10 shows the power consumption of all the transmission schemes presented in the paper. Circuit power values required by CM and MEM are characterized by very high consumptions, rapidly increasing towards the KW scale. On the other hand, the proposed technique shows low power consumption values which lie below the full system approaches, requiring $\sim$ $6.2W$ less than the MF without selection for the case studied by our simulations, i.e. when $N = 100$, $K = 5$ and $N_s = 5$.

Fig.11 is presented to clarify the benefits introduced by the proposed technique by showing the power savings $\zeta = P/P_{CI}$ over a M-MIMO system that involves CI, where P represents the power consumption of the studied technique and P_{CI} is used to identify the power required by the full system with CI. For the sake of simplicity we consider the same scenario, where $K = 5$, $N_s = 5$ and the RF chains power values are modeled as in (52). From Fig.11 it is clear that the proposed technique MF-CIM is less affected by the increased number of antennas at the transmitter because of the low complexity of the selection technique, since ζ decreases significantly as we increase N. In particular, we can notice a power saving of $\zeta = 0.38$ for the scenario used in our simulations, where $N = 100$, $K = 5$ and $N_s = 5$ with BPSK transmission, meaning that the performances are achieved with $\sim$ 62% less power. At the same time, we can see how the other low-complexity approach SM is characterized by increasing levels of power consumption at the base station, since the curves for both MF and CI present values that grow towards the equal consumption $\zeta = 1$ threshold as the array size at the BS N increases.

VIII. Conclusions

In this paper, we proved that antenna selection and constructive inter channel interference concepts can be jointly used to improve power efficiency performances of modern M-MIMO systems. We showed through analytical and numerical studies that we can optimize constructive interference at the receiver side by efficiently identifying a subset of antennas at the BS. We evaluated performances in terms of symbol error rate and a novel power efficiency metric, which combines throughput and power requirements to analyze the trade-offs introduced by the proposed scheme. We further characterized the presented system by confirming the numerical results through the derivation of a closed form expression of the SER, when received SINR is considered equal to its analytical upper-bound.

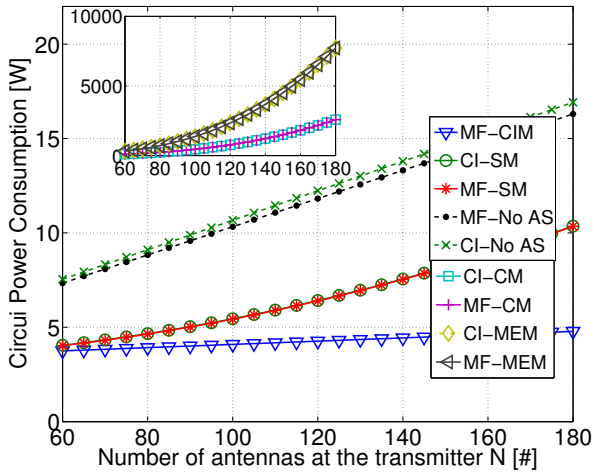

Fig. 10. Circuit power consumption at the BS as a function of the arrays size N for a system with $K = 5$ mobile stations and $N_s = 5$.

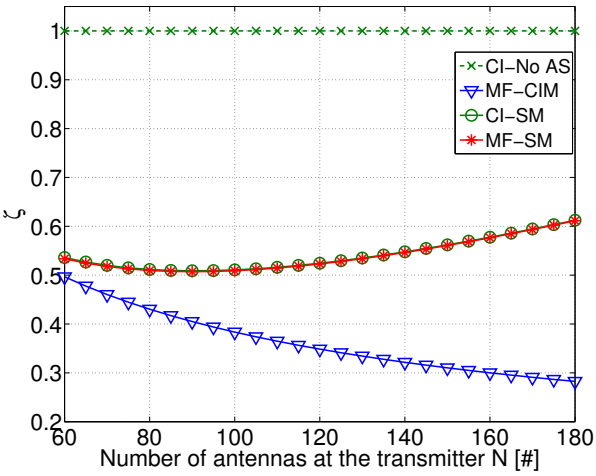

Fig. 11. RF Power Savings ζ as a function of the arrays size N at the transmitter for a system with $K = 5$ mobile stations and $N_s = 5$.

Acknowledgment

The authors wish to thank Marco Di Renzo for his help and insightful comments on fast RF switching.

References

[1] Q. Spencer, C. Peel, A. Swindlehurst, and M. Haardt, "An introduction to the multi-user MIMO downlink," *IEEE Communications Magazine*, vol. 42, no. 10, pp. 60–67, October 2004.

[2] E. Larsson, O. Edfors, F. Tufvesson, and T. L. Marzetta, "Massive MIMO for next generation wireless systems," *IEEE Communications Magazine*, vol. 52, no. 2, pp. 186–195, February 2014.

[3] F. Rusek, D. Persson, B. K. Lau, E. Larsson, T. Marzetta, O. Edfors, and F. Tufvesson, "Scaling up MIMO: Opportunities and challenges with Very Large Arrays," *IEEE Signal Processing Magazine*, vol. 30, no. 1, pp. 40–60, January 2013.

[4] T. L. Marzetta, "Noncooperative cellular wireless with unlimited numbers of base station antennas," *IEEE Transactions on Wireless Communications*, vol. 9, no. 11, pp. 3590–3600, November 2010.

[5] C. Masouros, M. Sellathurai, and T. Ratnarajah, "Large-Scale MIMO transmitters in fixed physical spaces: The effect of transmit correlation and mutual coupling," *IEEE Transactions on Communications*, vol. 61, no. 7, pp. 2794–2804, July 2013.

[6] C. Masouros and M. Matthaiou, "Space-Constrained Massive MIMO: Hitting the wall of favorable propagation," *IEEE Communications Letters*, vol. 19, no. 5, pp. 771–774, May 2015.

[7] J. Hoydis, S. ten Brink, and M. Debbah, "Massive MIMO: How many antennas do we need?" *2011 49th Annual Allerton Conference on Communication, Control, and Computing (Allerton)*, pp. 545–550, September 2011.

[8] H. Ngo, E. Larsson, and T. Marzetta, "Energy and spectral efficiency of very large multiuser MIMO systems," *IEEE Transactions on Communications*, vol. 61, no. 4, pp. 1436–1449, April 2013.

[9] L. Correia, D. Zeller, O. Blume, D. Ferling, Y. Jading, I. Godor, G. Auer, and L. Van der Perre, "Challenges and enabling technologies for energy aware mobile radio networks," *IEEE Communications Magazine*, vol. 48, no. 11, pp. 66–72, November 2010.

[10] A. Molisch and M. Win, "MIMO Systems with antenna selection," *IEEE Microwave Magazine*, vol. 5, pp. 46–56, March 2004.

[11] S. Sanayei and A. Nosratinia, "Antenna selection in MIMO systems," *IEEE Communications Magazine*, vol. 42, no. 10, pp. 68–73, October 2004.

[12] T. Gucluoglu and T. Duman, "Performance analysis of transmit and receive antenna selection over flat fading channels," *Wireless Communications, IEEE Transactions on*, vol. 7, no. 8, pp. 3056–3065, August 2008.

[13] A. Gorokhov, D. Gore, and A. Paulraj, "Receive antenna selection for MIMO spatial multiplexing: Theory and algorithms," *IEEE Transactions on Signal Processing*, vol. 51, no. 11, pp. 2796–2807, November 2003.

[14] A. Molisch, M. Win, and J. Winters, "Capacity of mimo systems with antenna selection," *IEEE International Conference on Communications*, vol. 2, pp. 570–574, 2001.

[15] Z. Chen, J. Yuan, B. Vucetic, and Z. Zhou, "Performance of alamouti scheme with transmit antenna selection," *Electronics Letters*, vol. 39, no. 23, pp. 1666–1668, November 2003.

[16] Z. Chen, J. Yuan, and B. Vucetic, "Analysis of transmit antenna selection/maximal-ratio combining in Rayleigh fading channels," *IEEE Transactions on Vehicular Technology*, vol. 54, no. 4, pp. 1312–1321, July 2005.

[17] R. Heath and A. Paulraj, "Antenna selection for spatial multiplexing systems based on minimum error rate," *IEEE International Conference on Communications (ICC)*, vol. 7, pp. 2276–2280, 2001.

[18] R. Chen, R. W. Heath, and J. G. Andrews, "Transmit selection diversity for unitary precoded multiuser spatial multiplexing systems with linear receivers," *IEEE Transactions on Signal Processing*, vol. 55, no. 3, pp. 1159–1171, March 2007.

[19] K. Dong, N. Prasad, X. Wang, and S. Zhu, "Adaptive antenna selection and Tx/Rx beamforming for large-scale MIMO systems in 60 GHz channels," *EURASIP Journal on Wireless Communications*, vol. 2011, no. 59, August 2011.

[20] B. Tae-Won and J. Bang Chul, "A practical antenna selection technique in multiuser massive MIMO networks," *IEICE Transactions on Communications*, vol. E96.B, no. 11, pp. 2901–2905, 2013.

[21] X. Gao, O. Edfors, J. Liu, and F. Tufvesson, "Antenna selection in measured massive MIMO channels using convex optimization," *2013 IEEE Globecom Workshops (GLOBECOM)*, pp. 129–134, 2013.

[22] H. Li, L. Song, and M. Debbah, "Energy efficiency of large-scale multiple antenna systems with transmit antenna selection," *IEEE Transactions on Communications*, vol. 62, no. 2, pp. 638–647, February 2014.

[23] B. M. Lee, J. Choi, J. Bang, and B.-C. Kang, "An energy efficient antenna selection for large scale green mimo systems," *IEEE International Symposium on Circuits and Systems (ISCAS)*, pp. 950–953, May 2013.

[24] S. Mahboob, R. Ruby, and V. Leung, "Transmit antenna selection for downlink transmission in a massively distributed antenna system using convex optimization," *International Conference on Broadband, Wireless Computing, Communication and Applications (BWCCA)*, pp. 228–233, November 2012.

[25] C. Masouros and E. Alsusa, "Dynamic linear precoding for the exploitation of known interference in MIMO broadcast systems," *IEEE Transactions on Wireless Communications*, vol. 8, no. 3, pp. 1396–1404, March 2009.

[26] ——, "Soft linear precoding for the downlink of DS/CDMA communication systems," *IEEE Transactions on Vehicular Technology*, vol. 59, no. 1, pp. 203–215, January 2010.

[27] C. Masouros, "Correlation rotation linear precoding for MIMO broadcast communications," *IEEE Transactions on Signal Processing*, vol. 59, no. 1, pp. 252–262, January 2011.

[28] C. Masouros, T. Ratnarajah, M. Sellathurai, C. Papadias, and A. Shukla, "Known interference in the cellular downlink: a performance limiting factor or a source of green signal power?" *IEEE Communications Magazine*, vol. 51, no. 10, pp. 162–171, October 2013.

[29] G. Zheng, I. Krikidis, C. Masouros, S. Timotheou, D. A. Toumpakaris, and Z. Ding, "Rethinking the role of interference in wireless networks," *IEEE Communications Magazine*, vol. 52, no. 11, pp. 152–158, November 2014.

[30] H. Yang and T. L. Marzetta, "Performance of conjugate and zero-forcing beamforming in Large-Scale Antenna systems," *IEEE Journal on Selected Areas in Communications*, vol. 31, no. 2, pp. 172–179, February 2013.

[31] M. Joham, W. Utschick, and J. Nossek, "Linear transmit processing in MIMO communications systems," *IEEE Transactions on Signal Processing*, vol. 53, no. 8, pp. 2700–2712, August 2005.

[32] C. Peel, B. Hochwald, and A. Swindlehurst, "A vector-perturbation technique for near-capacity multiantenna multiuser communication - Part I: Channel inversion and regularization," *IEEE Transactions on Communications*, vol. 53, no. 1, pp. 195–202, January 2005.

[33] A. H. Mehana and A. Nosratinia, "Diversity of MIMO linear precoding," *IEEE Transactions on Information Theory*, vol. 60, no. 2, pp. 1019–1038, February 2014.

[34] P.-H. Lin and S.-H. Tsai, "Performance analysis and algorithm designs for transmit antenna selection in linearly precoded multiuser MIMO systems," *IEEE Transactions on Vehicular Technology*, vol. 61, no. 4, pp. 1698–1708, May 2012.

[35] A. Müller, A. Kammoun, E. Björnson, and M. Debbah, "Linear precoding based on polynomial expansion : Reducing complexity in massive MIMO (extended version)," *IEEE Transactions on Signal Processing*, 2013, Submitted.

[36] S. Boyd and L. Vandenberghe, *Convex optimization*. Cambridge University Press, 2004.

[37] T. L. Marzetta, "How much training is required for multiuser MIMO?" *Asilomar Conference on Signals, Systems and Computers (ACSSC)*, pp. 359–363, October 2006.

[38] J. W. Demmel, *Applied numerical linear algebra*. Society for Industrial and Applied Mathematics, 1997.

[39] A. Pitarokoilis, S. Mohammed, and E. Larsson, "On the optimality of single-carrier transmission in Large-Scale Antenna systems," *IEEE Wireless Communications Letters*, vol. 1, no. 4, pp. 276–279, August 2012.

[40] S. Mohammed and E. Larsson, "Per-Antenna constant envelope precoding for large Multi-User MIMO systems," *IEEE Transactions on Communications*, vol. 61, no. 3, pp. 1059–1071, March 2013.

[41] C. Campbell and D. Dumka, "Wideband high power gan on sic spdt switch mmics," *IEEE MTT-S International Microwave Symposium Digest (MTT)*, pp. 1–1, May 2010.

[42] "Agilent solid state switches (White paper)," *Application Note*, 2010.

[43] M. Di Renzo, D. De Leonardis, F. Graziosi, and H. Haas, "Space Shift Keying (SSK) MIMO with practical channel estimates," *IEEE Transactions on Communications*, vol. 60, no. 4, pp. 998–1012, April 2012.

[44] J. Ney da Silva and M. de Campos, "Spectrally efficient UWB pulse shaping with application in orthogonal PSM," *IEEE Transactions on Communications*, vol. 55, no. 2, pp. 313–322, February 2007.

[45] B. Parr, B. Cho, K. Wallace, and Z. Ding, "A novel ultra-wideband pulse design algorithm," *IEEE Communications Letters*, vol. 7, no. 5, pp. 219–221, May 2003.

[46] X. Wu, Z. Tian, T. Davidson, and G. Giannakis, "Optimal waveform design for UWB radios," *IEEE Transactions on Signal Processing*, vol. 54, no. 6, pp. 2009–2021, June 2006.

[47] A. Mohammadi and F. Ghannouchi, "Single RF front-end MIMO transceivers," *IEEE Communications Magazine*, vol. 49, no. 12, pp. 104–109, December 2011.

[48] M. Di Renzo, H. Haas, A. Ghrayeb, S. Sugiura, and L. Hanzo, "Spatial Modulation for generalized MIMO: Challenges, opportunities, and implementation," *Proceedings of the IEEE*, vol. 102, no. 1, pp. 56–103, January 2014.

[49] O. N. Alrabadi, C. B. Papadias, A. Kalis, and R. Prasad, "A universal encoding scheme for mimo transmission using a single active element for psk modulation schemes," *IEEE Transactions on Wireless Communications*, vol. 8, no. 10, pp. 5133–5142, September 2009.

[50] N. Serafimovski, A. Younis, R. Mesleh, P. Chambers, M. Di Renzo, C.-X. Wang, P. Grant, M. Beach, and H. Haas, "Practical implementation of spatial modulation," *IEEE Transactions on Vehicular Technologies*, vol. 62, no. 9, pp. 4511–4523, November 2013.

[51] J. Perruisseau-Carrier, O. Alrabadi, and A. Kalis, "Implementation of a reconfigurable parasitic antenna for beam-space bpsk transmissions,"

European Microwave Conference (EuMC), pp. 644–647, September 2010.
[52] A. M. Tulino and S. Verdu, "Random matrix theory and wireless communications," *Foundations and Trends in Communications and Information Theory*, vol. 1, no. 1, pp. 1–182, June 2004.
[53] S. M. Razavi, T. Ratnarajah, and C. Masouros, "Transmit-power efficient linear precoding utilizing known interference for the multiantenna downlink," *IEEE Transactions on Vehicular Technology*, vol. PP, no. 99, pp. 1–12, 2014.
[54] C. Masouros, M. Sellathurai, and T. Ratnarajah, "Vector perturbation based on symbol scaling for limited feedback MISO downlinks," *IEEE Transactions on Signal Processing*, vol. 62, no. 3, pp. 562–571, February 2014.
[55] ——, "Computationally efficient vector perturbation precoding using thresholded optimization," *IEEE Transactions on Communications*, vol. 61, no. 5, pp. 1880–1890, May 2013.
[56] D. Ha, K. Lee, and J. Kang, "Energy efficiency analysis with circuit power consumption in massive MIMO systems," *IEEE 24th International Symposium on Personal Indoor and Mobile Radio Communications (PIMRC)*, pp. 938–942, September 2013.

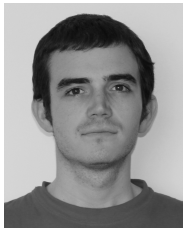

Pierluigi Vito Amadori (S'14), received the M.Sc. degree with honours in telecommunications engineering from the University of Rome La Sapienza, Rome, Italy, in 2013. Between 2012 and 2013 he held a JPL Visiting Student Researchers Program position in the Jet Propulsion Laboratory Pasadena, CA (USA). He is currently pursuing the Ph.D. degree in the Department of Electrical & Electronic Engineering at University College London, London, U.K. His main research interests include wireless communications with emphasis on large antenna array systems and energy efficient communications.

Christos Masouros (M'06, SM'14), is currently a Lecturer in the Dept. of Electrical & Electronic Eng., University College London. He received his Diploma in Electrical & Computer Engineering from the University of Patras, Greece, in 2004, MSc by research and PhD in Electrical & Electronic Engineering from the University of Manchester, UK in 2006 and 2009 respectively. He has previously held a Research Associate position in University of Manchester, UK and a Research Fellow position in Queen's University Belfast, UK.

He holds a Royal Academy of Engineering Research Fellowship 2011-2016 and is the principal investigator of the EPSRC project EP/M014150/1 on large scale antenna systems. His research interests lie in the field of wireless communications and signal processing with particular focus on Green Communications, Large Scale Antenna Systems, Cognitive Radio, interference mitigation techniques for MIMO and multicarrier communications. He is an Associate Editor for IEEE Communications Letters.